J Neurophysiol 98: 3770–3779, 2007.
First published September 26, 2007; doi:10.1152/jn.00850.2007.

New Angles on Neuronal Dendrites In Vivo

Werner Göbel and Fritjof Helmchen
Department of Neurophysiology, Brain Research Institute, University of Zurich, Zurich, Switzerland

Submitted 31 July 2007; accepted in final form 24 September 2007

Göbel W, Helmchen F. New angles on neuronal dendrites in vivo. *J Neurophysiol* 98: 3770–3779, 2007. First published September 26, 2007; doi:10.1152/jn.00850.2007. Imaging technologies are well suited to study neuronal dendrites, which are key elements for synaptic integration in the CNS. Dendrites are, however, frequently oriented perpendicular to tissue surfaces, impeding in vivo imaging approaches. Here we introduce novel laser-scanning modes for two-photon microscopy that enable in vivo imaging of spatiotemporal activity patterns in dendrites. First, we developed a method to image planes arbitrarily oriented in 3D, which proved particularly beneficial for calcium imaging of parallel fibers and Purkinje cell dendrites in rat cerebellar cortex. Second, we applied free linescans—either through multiple dendrites or along a single vertically oriented dendrite—to reveal fast dendritic calcium dynamics in neocortical pyramidal neurons. Finally, we invented a ribbon-type 3D scanning method for imaging user-defined convoluted planes enabling simultaneous measurements of calcium signals along multiple apical dendrites. These novel scanning modes will facilitate optical probing of dendritic function in vivo.

INTRODUCTION

Most neurons in the mammalian CNS possess elaborate dendrites forming numerous synaptic contacts with their presynaptic partners. With their diverse morphological and physiological features dendrites are essential for synaptic integration in single neurons and for signal processing in neuronal circuits (Häusser et al. 2000; Yuste and Tank 1996). A key function of dendrites is to spatially confine electrical and biochemical signals. Such compartmentalization occurs on multiple levels ranging from dendritic spines (Yuste et al. 2000) to dendritic arbors that might act as nonlinear thresholding units for local integration of synaptic potentials (Polsky et al. 2004). The dendritic distribution of intracellular calcium ion concentration changes is particularly relevant because calcium ions are a key regulator of synaptic plasticity (Häusser et al. 2000; Holthoff et al. 2006). Measurements of the spatiotemporal dynamics of dendritic excitation therefore are crucial for further understanding of dendritic integration, synaptic plasticity, and neural network function.

Although dendritic function can be directly probed using electrical recordings with micropipettes (Stuart and Spruston 1995) this approach permits simultaneous recordings from a few locations at most. Alternatively, various imaging techniques have been applied to characterize spatiotemporal activity patterns in dendrites including camera systems and laser-scanning microscopes (Häusser et al. 2000; Yuste and Tank 1996). Two-photon microscopy (Denk et al. 1990) has the particular advantage that it enables calcium imaging from dendrites in the mammalian brain in vivo (Svoboda et al. 1997; reviewed in Helmchen and Waters 2002). It has been difficult though to simultaneously image large parts of dendritic trees in the intact brain because many dendrites are oriented "vertically," with their main axis perpendicular to the tissue surface and thus to the conventional *x*–*y*-imaging plane. As a consequence in vivo measurements from dendrites in the neocortex (Helmchen et al. 1999; Svoboda et al. 1997, 1999; Waters and Helmchen 2004; Waters et al. 2003), the olfactory bulb (Charpak et al. 2001; Debarbieux et al. 2003), and the cerebellum (Sullivan et al. 2005) have been restricted to selective and sequential sampling from dendritic cross sections.

Novel approaches for more comprehensive imaging of dendritic activity in vivo are desirable, particularly in view of the recent advances in calcium indicator labeling (Heim et al. 2007; Kerr et al. 2005; Nagayama et al. 2007; Nevian and Helmchen 2007; Stosiek et al. 2003). New scanning technologies and strategies for two-photon microscopy (Iyer et al. 2006; Kurtz et al. 2006; Nguyen et al. 2001; Salome et al. 2006) so far aimed at fast imaging in a single plane rather than from arbitrarily oriented structures. Recently, we introduced a simple three-dimensional (3D) laser-scanning method, which is based on a 3D scan trajectory created by galvanometric scan mirrors in combination with a piezoelectric focusing device (Göbel et al. 2007). This approach enables optical recordings from large cell populations in 3D space. Here, we present several additional 3D laser-scanning modes that are especially advantageous for imaging dendritic excitation in vivo. For the first time we demonstrate imaging of dynamic signaling in dendrites of cerebellar Purkinje cells and neocortical pyramidal neurons with viewing angles as if the observer were sitting inside the intact brain.

METHODS

Animal preparation and fluorescence staining

All experiments were carried out according to the guidelines of the Center for Laboratory Animals of the University of Zurich and were approved by the Cantonal Veterinary Office. We anesthetized Wistar rats (16–28 days old) with urethane (1.5 g/kg body weight) and performed a craniotomy above somatosensory cortex or cerebellum as described (Sullivan et al. 2005; Waters et al. 2003). We carefully removed the dura and superfused the exposed brain with normal rat Ringer (NRR) solution (in mM: 135 NaCl, 5.4 KCl, 5 HEPES, 1.8 $CaCl_2$; pH 7.2 with NaOH). To dampen heartbeat- and breathing-induced motion, we filled the cranial window with agarose (type III-A, Sigma; 1% in NRR) and covered it with an immobilized glass coverslip.

We achieved extracellular staining by bolus injection of the red fluorescent dye Alexa-594 (200 μM; Molecular Probes; diluted in NRR) through a micropipette positioned in cortical layer 2/3 or

Address for reprint requests and other correspondence: F. Helmchen, Dept. of Neurophysiology, Brain Research Institute, Winterthurerstr. 190, CH-8057 Zurich, Switzerland (E-mail: helmchen@hifo.uzh.ch).

The costs of publication of this article were defrayed in part by the payment of page charges. The article must therefore be hereby marked "*advertisement*" in accordance with 18 U.S.C. Section 1734 solely to indicate this fact.

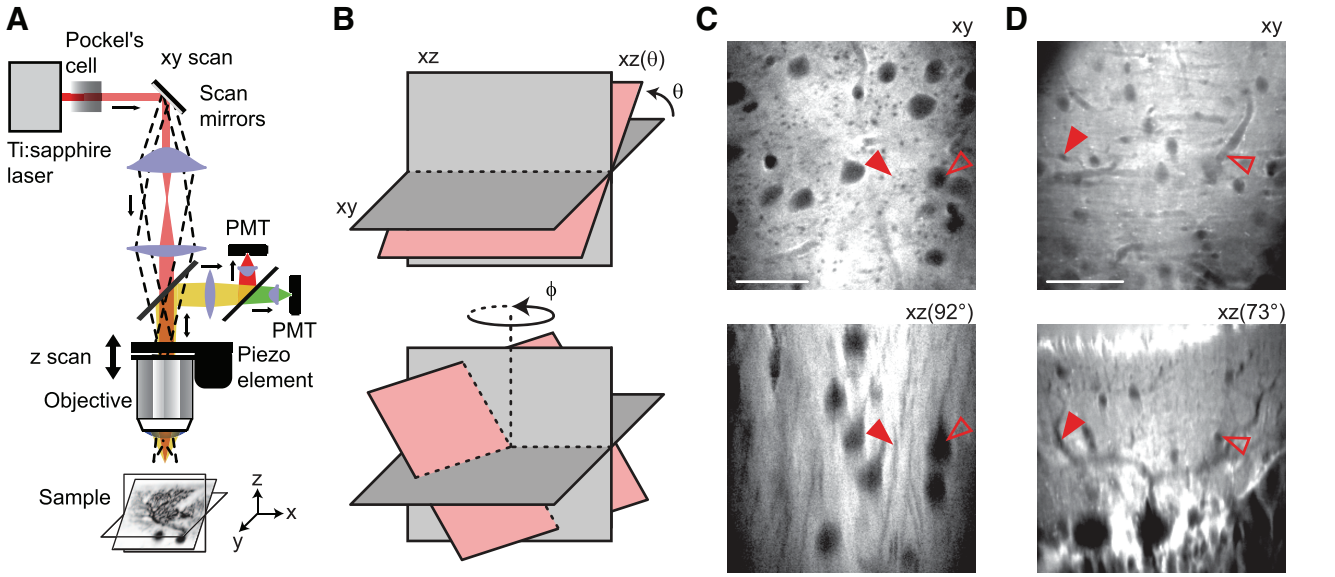

FIG. 1. Principle of arbitrary plane imaging in 3 dimensions (3D). *A*: 2-photon microscope setup. Two galvanometric mirrors are used for *x*–*y*-scanning and a piezoelectric focusing element for *z*-scanning. Laser intensity is adjusted with a Pockel's cell. Fluorescence is detected in 2 color channels using photomultipliers (PMTs). *B*: schematic of arbitrary plane scanning. Imaged plane can be tilted by an angle θ and freely rotated around the optical axis by ϕ. *C*: examples of vertical in vivo imaging in neocortical layer 2/3. Cellular structures were negatively stained by applying an extracellular stain. Standard *x*–*y* view is compared with the side view with the angle θ optimized to image dendritic structures. Arrowheads indicate a corresponding dendrite (solid marker) and soma (open marker) in top and side views. Scale bar: 40 μm. *D*: comparison of top and side views in the molecular layer of cerebellar cortex. A negatively stained Purkinje cell dendrite and a blood vessel are marked by a solid and open arrowhead, respectively. Scale bar: 40 μm.

cerebellar molecular layer, respectively. Population staining with a calcium indicator was performed using the multicell bolus loading technique (Stosiek et al. 2003). Briefly, the acetoxymethyl (AM) ester of Oregon Green-BAPTA-1 (OGB-1 AM; 50 μg; Molecular Probes) was dissolved in DMSO plus 20% Pluronic F-127 (BASF; Florham Park, NJ) and diluted in NRR to a final concentration of 1 mM. The dye was pressure ejected into the molecular layer of cerebellar cortex using a micropipette. For electrical stimulation of parallel fibers, current pulses (100 μs; 0.1–5 μA) were delivered through a glass pipette (~2-μm tip size) placed in molecular layer 200–400 μm distant from the imaging area. Alexa-594 (20 μM) was included in the pipette for visualization.

For loading subsets of neurons in neocortex or cerebellum with calcium indicator we adopted the recently introduced method of local electroporation (Nagayama et al. 2007). A micropipette (~2-μm tip size) was filled with a high concentration (30 mM) of Oregon Green BAPTA-1 (OGB-1; diluted in NRR). After positioning the pipette in cortical layer 3 or in the molecular layer of cerebellar cortex we applied a series of current pulses at 2 Hz (5 μA; 25-ms pulse width; 1,200–2,400 pulses in total). Typically 5–15 neurons were stained with calcium indicator dye within 15 min. Washing the brain surface with NRR removed most of the remaining extracellular stain.

Two-photon laser-scanning microscopy

We used a custom-built two-photon microscope with approximately 100-fs-long laser pulses at 870-nm wavelength provided by a Ti:sapphire laser system (Tsunami and Millenia-X; Spectra-Physics). We adjusted beam size with a telescope and modulated laser intensity with a Pockel's cell (Conoptics). We used two galvanometric scan mirrors (model 6210; Cambridge Technologies) for *x*–*y*-scanning and a piezoelectric focusing element (P-725.4CD PIFOC, Physik Instrumente) with ≤400 μm travel in closed-loop mode for rapid *z*-scanning along the optical axis (Fig. 1*A*; Göbel et al. 2007). In all experiments, we used a water-immersion objective (40× LUMPlanFl/IR, 0.8 NA; Olympus) and acquired fluorescence images with laser-scanning software custom-written in the LabVIEW environment (National Instruments). We incorporated the novel axial scanning modes in our LabVIEW program.

ARBITRARY PLANE IMAGING. For arbitrary plane imaging the *x*–*y*–*z*-scan signals were subject to two coordinate transformations: first a rotation around the *x*-axis by an angle θ followed by a rotation around the *z*-axis (the optical axis) by ϕ (Fig. 1*B*). Mathematically, we applied two rotation matrices

$$\begin{bmatrix} x_i(\theta,\phi) \\ y_i(\theta,\phi) \\ z_i(\theta,\phi) \end{bmatrix} = \begin{bmatrix} \cos\phi & -\sin\phi & 0 \\ \sin\phi & \cos\phi & 0 \\ 0 & 0 & 1 \end{bmatrix} \begin{bmatrix} 1 & 0 & 0 \\ 0 & \cos\theta & -\sin\theta \\ 0 & \sin\theta & \cos\theta \end{bmatrix} \begin{bmatrix} x_i(0) \\ y_i(0) \\ z_i(0) \end{bmatrix} \quad (i = 1 \cdots n) \quad (1)$$

where $x_i(0)$, $y_i(0)$, and $z_i(0)$ denote the vector components of the initial horizontal *x*–*y*-scan pattern [$x_i(0)$ represents the fast linescan signal, $y_i(0)$ the sawtooth-like slow scan signal, and $z_i(0)$ equals 0 for all *n* initial vectors]. To ensure equal image dimensions in all spatial directions the *z*-scan signal was multiplied with a constant factor σ. In addition, a constant offset τ was added so that the objective was centered at the middle position of the *z*-range of the piezoelectric focus (in our case 200 μm)

$$z_{final,i}(\theta,\phi) = \sigma \cdot z_i(\theta,\phi) + \tau \quad (2)$$

These transformations enabled θ rotations around the midline of the *x*–*y*-image. Coordinate transformations could be applied on-the-fly in the focusing mode and a hot key permitted rapid back-and-forth switching between the *x*–*y*- and *x*–*z*-views.

2D FREE LINESCAN. We used our previously described point insertion algorithm (Göbel et al. 2007) to generate a smooth user-defined linescan in a horizontal plane. Briefly, preselected points of interest were appropriately sorted and novel points were iteratively added in between so that a closed, smoothly curved line was obtained passing

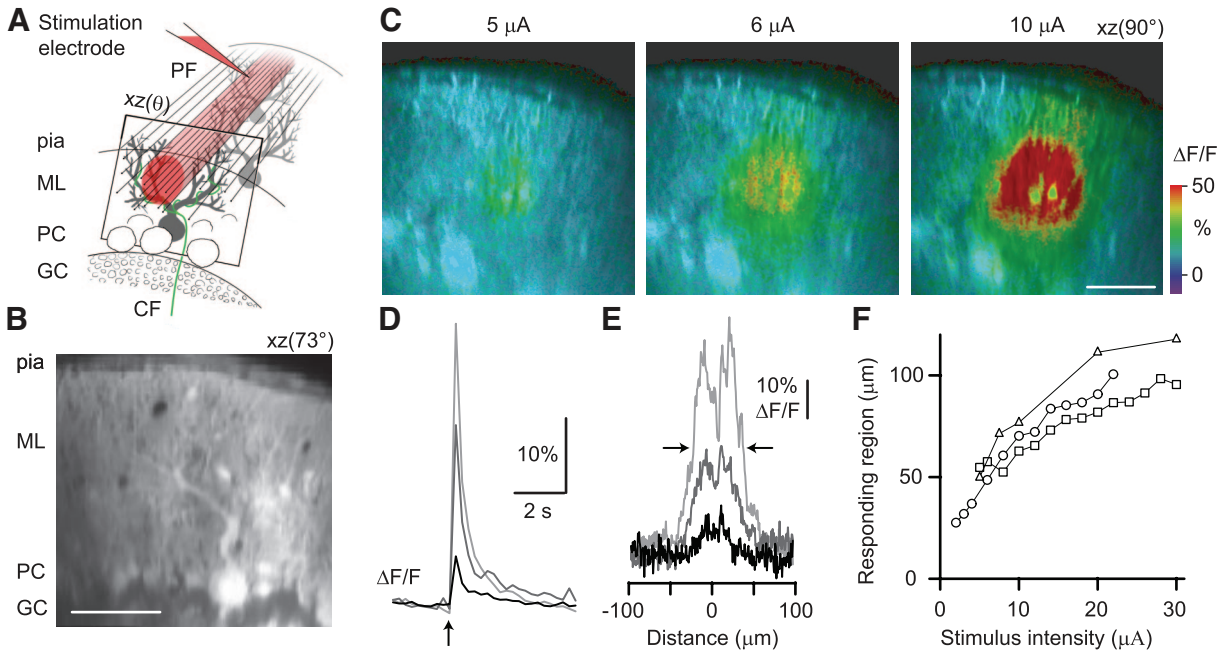

FIG. 2. Live imaging of parallel fiber beams in the cerebellar cortex. *A*: schematic of *x–z* imaging in cerebellar cortex. Electrical stimulation with a distant electrode excites bundles of parallel fibers (PFs; red) that make synaptic contact onto perpendicularly oriented Purkinje cell dendrites (gray). Purkinje cells receive additional synaptic input from climbing fibers (CFs). *B*: sagittal fluorescence image following bolus loading with the calcium indicator Oregon Green BAPTA-1 (OGB-1) AM (acetoxymethyl ester). Image orientation was aligned with the major branch of a Purkinje cell dendrite. Molecular layer (ML), Purkinje cell (PC), and granule cell (GC) layer are discernible. Scale bar: 50 μm. *C*: 3 examples of snapshots of cross-sectional activation of PF beams at different stimulation intensities. Images were taken at the peak of the calcium transients. Scale bar: 50 μm. *D*: time course of the calcium transients in the center of the PF beam for the 3 examples shown in *C*. *E*: spatial profile of the PF beam through the center of the PF beam at 3 different stimulus intensities. Same responses as in *D*. *F*: increase of the diameter (full-width half-maximum) of the responding region with stimulus intensity in 3 different experiments.

through all selected points. From this set of 2D scan vectors a new set was then calculated using our pixel redistribution algorithm (Göbel et al. 2007) so that the final scan points $\vec{S}_i = (x_i, y_i)$ $(i = 1 \ldots n)$ were equidistantly spaced along the free linescan where n is the number of points per line as defined by the user.

3D FREE LINESCAN. To create a 3D scan trajectory along a single apical dendrite we used our recently introduced user-defined 3D linescan method (Göbel et al. 2007). In this mode, the microscope objective is set into sinusoidal motion along the optical axis (frequency 20 Hz). The cross section of a single dendrite was marked at different focal depths based on a previously acquired reference image stack. Constrained by the sinusoidal movement of the objective we then calculated a smooth scan line passing through the preselected set of points along the dendrite. Because of the inertia of the piezoelectric focusing element plus objective load the actual z-position of the objective in general does not accurately match the imposed drive signals. For a sinusoidal motion, a frequency-dependent amplitude reduction and phase shift result, which need to be corrected. To this end we first determined the phase shift and amplitude reduction by comparing the original drive signals with the resulting position feedback signals. Then, the drive signal was negatively phase shifted by the determined angle and multiplied by the amplitude-reduction factor (Göbel et al. 2007). Due to a deviation of the z-motion from a sinusoid at 20 Hz, however, a complete correction was not possible. Although this problem impeded accurate vertical scanning along the entire dendrite, we could always assign the measured signals to dendritic segments based on the position-feedback signals from the piezoelectric focusing element and the reference image stack.

3D RIBBON SCANNING. For 3D ribbon scanning we selected the cross sections of multiple dendrites (using the same order) in two horizontal *x–y* planes at focal depths z_1 and z_2 and calculated two 2D free linescans $\vec{S}_i^1$ and $\vec{S}_i^2$ at z_1 and z_2, respectively $(i = 1 \ldots n$ for both sets of points with n denoting the number of pixels for the scan trajectories). We then calculated a full 3D ribbon scan pattern by linearly interpolating $\vec{S}_i^1$ and $\vec{S}_i^2$

$$\vec{R}_{i,j} = \vec{S}_i^1 + \frac{i}{j}(\vec{S}_j^2 - \vec{S}_i^1) \quad (3)$$

where $j = 0 \ldots (n - 1)$ (with i = constant) and $i = 0 \ldots (n - 1)$. We implemented vertical motion of the objective between focal planes z_1 and z_2 by using a sawtooth-like z-signal. A sinusoidal z-motion would be equally possible. Because of the low z-scanning frequency (maximally 8 Hz) amplitude reduction was negligible and only small phase shift corrections were necessary.

LASER INTENSITY ADJUSTMENT. Assuming an exponential decrease of two-photon excitation with focal depth due to light scattering (Kleinfeld et al. 1998) we compensated excitation loss by modulating the Pockel's cell according to

$$I(\Delta z) = I(0)e^{\Delta z/\lambda} \quad (4)$$

where λ denotes the scattering length for the excitation light, $I(0)$ is the intensity used at the initial *x–y* plane, and Δz is the axial deviation from this plane. For example, in the arbitrary plane imaging mode the image is tilted by rotation around the midline of the initial *x–y* image. Excitation intensity is decreased for those parts of the tilted image that lie above the initial plane ($z < 0$) and increased for the parts below ($z > 0$). The scattering length was empirically adjusted during imaging until a rather homogeneous illumination of the tilted image was achieved. In our experiments, we used λ-values between 200 and 250 μm with no apparent difference for neocortex and cerebellum.

Data analysis

We analyzed calcium signals in defined regions of interest (ROIs) as relative fluorescence changes (ΔF/F) after background subtraction. Decay time constants were obtained from exponential fits to calcium transients. For PF beams, we defined the responding region as full-width half-maximum of the spatial ΔF/F profiles through the center of the beam. We obtained ΔF/F images using ImageJ software by merging the average fluorescence image of an entire movie with the time series of fluorescence changes into a single HSB-color coded image. ΔF/F changes were appropriately mapped onto the *hue* (H) scale and were also partially used for the *saturation* (S) channel. The average intensity image was used for the *brightness* (B) channel. All results are given as means ± SD.

RESULTS

Arbitrary plane imaging in 3D space

A major challenge for imaging dendrites in vivo is their variable orientation in 3D space. In a first approach we devised a laser-scanning mode that permits imaging of arbitrary planes in three dimensions (Fig. 1*A*). We used a custom two-photon microscope with galvanometric scan mirrors for *x*–*y*-scanning and a piezoelectric focusing element for *z*-scanning (Göbel et al. 2007). By transferring part of the slow, sawtooth-like *y*-scan signal to the *z*-scan (using appropriate scaling to maintain image dimensions) the image plane could be rotated by an angle θ around the *x*-axis (Fig. 1*B*). In the extreme case (θ = 90°) the entire *y*-scan signal was transferred to the piezoelectric focus tilting the image plane to the vertical *x*–*z* plane. By implementing a second rotation around the *z*-axis by an angle ϕ we could arbitrarily choose the orientation of the image plane in 3D space (Fig. 1*B*). For imaging deep in biological tissue, the reduction of two-photon excitation with focal depth caused by light scattering has to be taken into account. We compensated changes in excitation intensity during *z*-scanning by automatic adjustment of the average laser power according to focal depth (see METHODS).

To demonstrate in vivo imaging of vertically oriented dendrites we applied a simple extracellular stain by bolus injection of the red fluorescent dye Alexa-594 into superficial layers of neocortex and cerebellar cortex of anesthetized rats (Fig. 1, *C* and *D*). In both brain regions cell bodies were clearly visible as negatively stained ("black") holes in the conventional *x*–*y* view. Smaller black spots between cell bodies indicated possible locations of dendritic cross sections (Fig. 1, *C* and *D*, *top images*). Rotation of the image plane allowed inspection of these structures under all possible orientations. More specifically, in neocortical tissue θ-rotation by values between 75 and 105° tilted the image plane so that it was aligned with apical dendrites that either emerged from layer 2/3 pyramidal cell bodies or apparently originated from deeper layers [Fig. 1*C*, *bottom image*; for all side views the specific tilt angle θ is given as *xz*(θ)]. Similarly, by appropriately choosing rotation angles the cross-sectional *x*–*y* view of the cerebellar cortex turned to a sagittal view so that the different layers were discernible and individual negatively stained Purkinje cells could be resolved including the main arbors of their dendritic tree (Fig. 1*D*, *bottom image*; see also supplemental movie 1).[1] Note that the spatial resolution generally depends on the effectively used NA and that the transformation to a sagittal view results in a lower spatial resolution in the *z*-direction because of the elongation of a diffraction-limited focus along the optical axis.

Because the travel range of the piezoelectric focus is 400 μm, we easily achieved fields of view of several-hundred-micrometer side length for all orientations. The temporal resolution of arbitrary plane scanning is similar to standard *x*–*y*-scanning (2–10 frames/s depending on the line duration

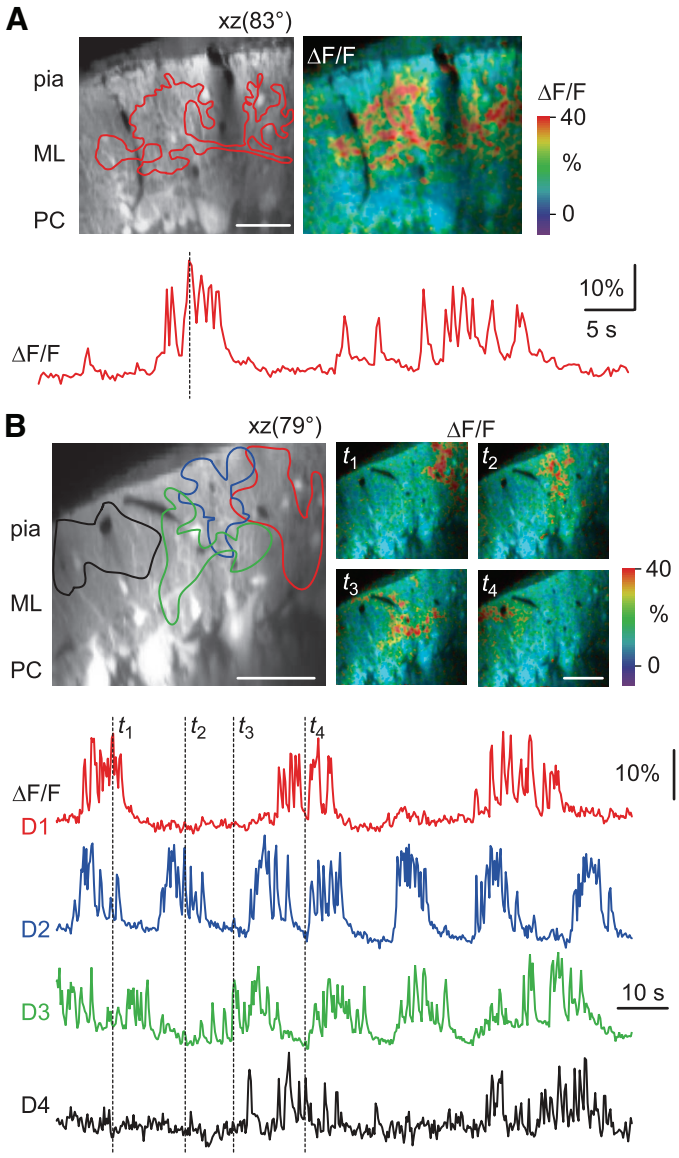

FIG. 3. Dendritic calcium signals in Purkinje cells in bulk-loaded tissue. *A*: side view of cerebellar cortex (*left*) and single ΔF/F image (*right*) from a time series of spontaneous activity (4-Hz frame rate). A region of interest (ROI) was defined around the activated region, which corresponds to the outline of one Purkinje cell dendrite. Soma of this Purkinje cell presumably was located outside the field of view. *Bottom trace*: time course of the relative fluorescence change in the ROI. Dashed vertical line indicates the time point of the ΔF/F image shown in the *top right*. Scale bar: 50 μm. *B*: similar experiment as in *A*. In this example 4 responsive regions were analyzed, which presumably correspond to dendrites of different Purkinje cells. *Bottom traces*: time course of the relative fluorescence change in the 4 ROIs. Dashed vertical lines indicate the time points of the snapshot ΔF/F images shown in the *top right*. Scale bar: 50 μm.

[1] The online version of this article contains supplemental data.

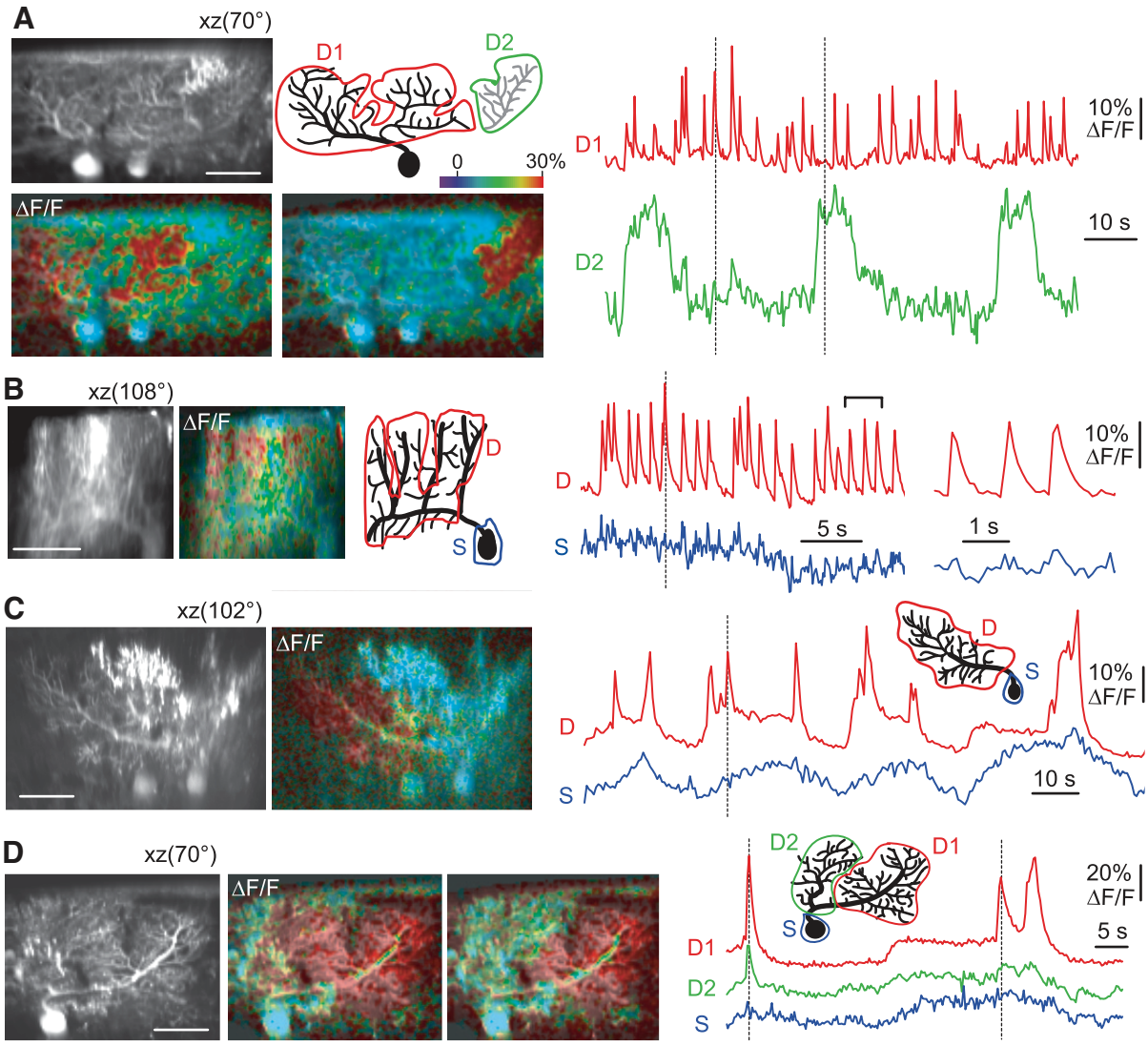

FIG. 4. In vivo calcium imaging of Purkinje cell dendrites. *A*, *left*: sagittal average fluorescence image of several labeled Purkinje cells following local electroporation (*top*). Two ΔF/F snapshot images from 2 different time points are shown below. A sketch of the regions of interest (ROIs) is shown in the *top right*. ROIs correspond to dendritic arbors from 2 different cells (D1 and D2). *Right*: time course of the relative fluorescence changes for D1 and D2. Vertical dashed lines indicate time points of the ΔF/F snapshots. Acquisition rate: 4 Hz. *B*: side view, ΔF/F snapshot, and ROI sketch for another cell. Time course of spontaneously occurring fluorescence changes is plotted to the *right* for a dendritic and a somatic ROI. Three calcium transients (brackets) are shown on an expanded timescale to show the decay time course. Acquisition rate: 10 Hz. *C*: side view, ΔF/F snapshot, and ROI sketch for a 3rd cell. In this cell slow modulations in the calcium signals were apparent in both the dendritic and the somatic ROI. Sharp calcium transients occurred in the dendritic ROI preferentially near the beginnings and the ends of plateaus. Acquisition rate: 2 Hz. *D*: side view of a 4th example cell. ΔF/F snapshot images are shown for 2 time points, for which the 2 dendritic arbor regions D1 and D2 displayed differential activation. Acquisition rate: 4 Hz. For all cells the tilt angle is given in brackets. Scale bar is 50 μm for all images.

and the number of lines). This novel scanning mode thus is excellently suited for functional imaging of structures that are anatomically arranged perpendicular to the brain surface.

Calcium imaging in the molecular layer of cerebellar cortex

We first used arbitrary plane imaging for functional measurements in the cerebellum. The molecular layer of cerebellar cortex has a well-defined anatomical organization with parallel fibers (PFs) running along the mediolateral axis, making numerous contacts with flat dendritic trees of Purkinje cells that lie in parasagittal sections (Fig. 2*A*). Multicell bolus loading (Stosiek et al. 2003) of the calcium indicator Oregon Green BAPTA-1 (OGB-1) resulted in unspecific staining of cell bodies and neuropil within a diameter of several hundred micrometers (Sullivan et al. 2005). In the axial view ($\theta \approx 90°$), the different layers of the cerebellar cortex were clearly distinguishable (Fig. 2*B*). We could hardly resolve individual cells in the granule cell layer though, presumably due to enhanced light scattering and laser beam distortion in the Purkinje cell layer. Because multiple cellular structures are labeled using bolus loading, we next aimed to isolate calcium signals in the various compartments.

Electrical stimulation in the molecular layer excites bundles of parallel fibers ("PF beams") that extend several hundred micrometers laterally (Pichitpornchai et al. 1994). Using arbitrary plane imaging, we could directly visualize PF beam cross sections in a sagittal view. We stimulated PFs with a micropipette inserted into the molecular layer 200–400 μm distant from the imaging site. Single stimuli evoked calcium transients confined to circularly shaped regions in the molecular layer (Fig. 2*C*; supplemental movie 2). Consistent with progressive recruitment of PFs, the peak amplitude and spatial extension of the calcium transients increased with stimulation intensity, whereas the time course did not change (Fig. 2, *D–F*; average decay time constant 578 ± 40 ms, $n = 3$ animals). These results are consistent with a previous in vivo study, in which sagittal views of PF beam cross sections were reconstructed from sequential linescan measurements at different focal depths (Sullivan et al. 2005).

Dendrites of single Purkinje cells lie within a 2D plane perpendicular to both the PF axis and the brain surface. In several experiments using bolus loading of calcium indicator we were able to identify the main dendritic arbors of Purkinje cells. Moreover, in sagittal views we observed spontaneous activity that apparently originated from Purkinje cell dendrites (Fig. 3*A*; supplemental movie 3). In three animals these putative Purkinje cell signals were characterized by brief calcium transients (decay time constant 354 ± 119 ms, $n = 7$ cells), in agreement with previous *x–y* measurements (Sullivan et al. 2005). Calcium transients either occurred rather regularly (mean frequency 0.39 ± 0.18 Hz, $n = 6$ cells) or were superimposed on slower oscillations on the timescale of 10–30 s (8 of 14 cells; Fig. 3*B*).

In vivo imaging of dendritic activity in Purkinje cells

To further examine dendritic activity in Purkinje cells we applied local electroporation as an alternative method to selectively label only a few Purkinje cells (Nagayama et al. 2007). Local electroporation of OGB-1 in the molecular layer resulted in dye loading of 3–22 Purkinje cells and also labeled a spatially restricted bundle of crossing PFs. Arbitrary plane scanning enabled calcium imaging in vertically oriented optical sections that contained dendrites of either a single or a few neighboring Purkinje cells (Fig. 4). As in the bolus loading experiments we observed variable spontaneous activity patterns in Purkinje cell dendrites of four animals. Nearly all dendrites exhibited fast calcium transients (mean frequency 0.67 ± 0.29 Hz, $n = 19$ cells). In 15 cells measured at high frame rates (≥4 Hz) the mean decay time constant was 266 ± 57 ms (Fig. 4*B*). Fast calcium transients were prominent in dendritic regions but absent or very small in somata when simultaneous measurements could be made (Fig. 4, *B–D*). These features suggest that calcium transients originated from dendritic calcium spikes that presumably were associated with complex spikes and triggered by climbing fiber activation (Keating and Thach 1997; Miyakawa et al. 1992; Sullivan et al. 2005). In about 25% of cells, in addition, we observed slow oscillations in the calcium signal with periods of enhanced activity (duration 2–30 s) alternating with more quiet periods. In the example in Fig. 4*C* large brief calcium transients preferentially occurred at the beginning and the end of such slow oscillations, which is reminiscent of the recently reported bistability of Purkinje cells in vivo and complex spike-induced transitions between "up" and "down" states (Loewenstein et al. 2005). In one experiment, two different dendritic arbors, which could clearly be assigned to the same Purkinje cell, were differentially activated (Fig. 4*D*; supplemental movie 4).

From these examples we conclude that arbitrary plane imaging is well suited to study calcium signaling in various components of the cerebellar cortex, particularly in Purkinje cell dendrites.

Horizontal and vertical free linescans resolve fast dendritic calcium signals

We further aimed at functional imaging of dendrites in the neocortex in vivo. Using local electroporation in layer 2/3 of somatosensory cortex we were able to load 5–10 neocortical pyramidal neurons with OGB-1. Although arbitrary plane imaging permitted sideways imaging of segments of the labeled apical dendrites (data not shown), the improvement provided by this mode was limited because vertically oriented planes contained two or three apical dendrites at most. We therefore devised additional scanning modes more suitable for measurements from pyramidal cell dendrites.

First, we applied user-defined free linescans in the horizontal plane to simultaneously measure fast calcium signals from multiple neighboring dendrites (Fig. 5). In the *x–y* view individual dendrites appeared as small, bright spots. Dendritic

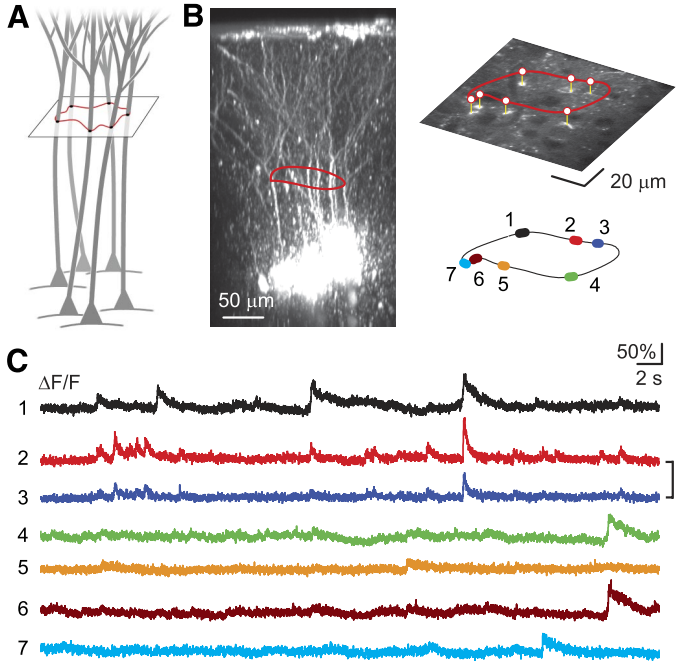

FIG. 5. Horizontal free linescan for fast measurements from multiple neocortical dendrites. *A*: schematic drawing of a subset of labeled neocortical pyramidal cells. Dendritic cross sections are selected in a particular focal plane and a curved, smooth scan trajectory (red) is defined. *B*, *left*: side view of labeled L2/3 neocortical cell population, stained with the calcium indicator OGB-1 using local electroporation 250–300 μm below the pia (not labeled cell bodies). A user-defined linescan is indicated in red. *Top right*: 2-photon fluorescence image with selected dendritic cross sections marked by vertical lines (yellow) and the resulting 2D linescan (red; slightly elevated). *Bottom right*: numbering and color code of the sampled dendrites. *C*: spontaneous calcium signals from the 9 selected dendrites. Color code corresponds to *B*. Note that synchronous activity occurred in some of the dendrites.

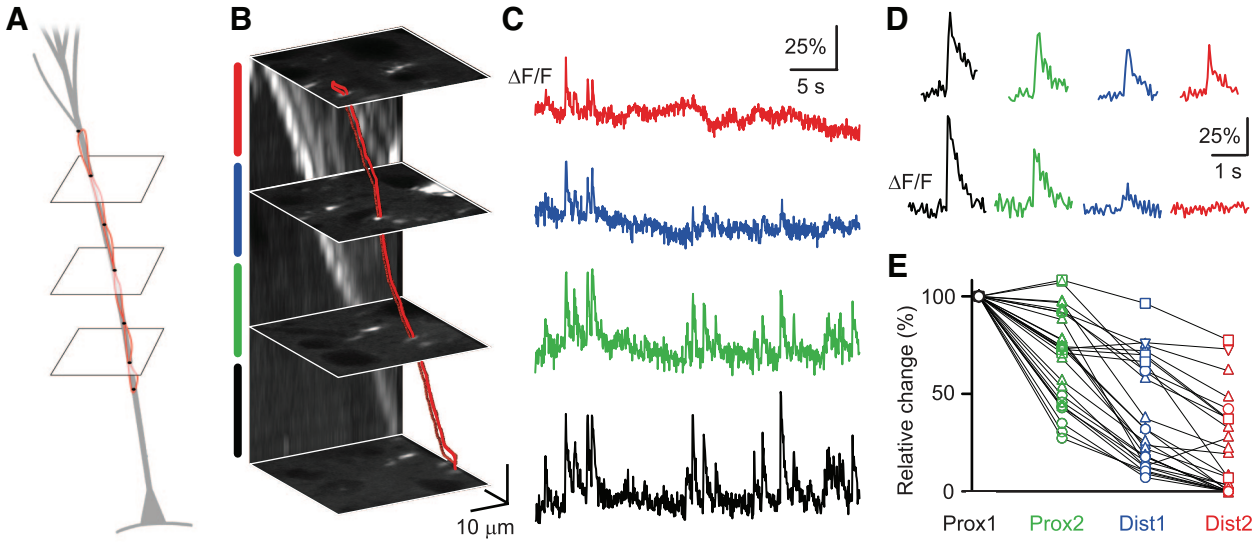

FIG. 6. Vertical linescan along a single dendrite. *A*: principle of user-defined vertical linescan. Scan trajectory (red) is calculated based on the selection of the dendritic cross section at different focal depths from a previously acquired reference image stack. *B*: example of a scan trajectory (red) along the distal portion of an apical dendrite of a pyramidal neuron filled with OGB-1 (100-μm z-range). Four cross-sectional planes are shown in addition to the side view of the dendrite. Dendritic segment covered by the scan line was divided into 2 proximal parts (black and green) and 2 distal parts (blue and red). *C*: spontaneous calcium transients in the 4 regions of the dendrite shown in *B*. Same color code as in *B*. Note the highly variable amplitude of calcium transients in the distal part of the dendrite. Decay time constants of exponential fits were 228 ± 101, 276 ± 122, 308 ± 70, and 317 ± 66 ms (mean ± SD) from proximal to distal. *D*, *top*: example of a calcium transient that spread far into the distal dendrite. *Bottom*: example of a highly attenuated calcium transient in the same recording. Same color code as in *B*. *E*: summary plot of the spatial profile of the calcium transient amplitude (normalized to the most proximal measurement). Different symbols correspond to different dendrites in 4 experiments.

cross sections were preselected and a smooth 2D scan trajectory was calculated passing through these points (Fig. 5, *A* and *B*; see METHODS). User-defined linescans provide excellent temporal resolution (≤1 kHz). In five experiments we measured spontaneously occurring fast calcium transients from multiple dendrites (Fig. 5*C*). This scanning mode thus is suitable for studying the distribution and synchrony of dendritic activation in subnetworks of pyramidal neurons.

Several important questions (such as where action potentials are initiated, how far they spread, and where synaptic inputs arrive) require measurements of the spatial profile of dendritic calcium transients. In a second approach, we therefore devised a method to scan along the vertically oriented dendrites of pyramidal neurons in vivo (Fig. 6). The method uses our recently introduced user-defined 3D linescan technique, which is based on the preselection of points of interest in a 3D volume (Göbel et al. 2007). Here, we applied this method to image the spatial profile of calcium signals in individual apical dendrites filled with OGB-1. Several points were selected from a reference image stack to define a vertically oriented free linescan trajectory along the dendrite (Fig. 6, *A* and *B*). To achieve fast z-scanning the objective was vibrated sinusoidally at 20 Hz, which requires compensation of amplitude reduction and phase shift (see METHODS). Because of remaining deviations from the desired path the dendrites typically were not followed accurately along the entire imaged segment. Nevertheless, fluorescence signals from dendritic sections at multiple focal depths could be analyzed.

In four experiments on distal apical dendrites (typically 100 μm downward from the main bifurcation and in one case 300 μm downward almost to the soma) we observed spontaneous calcium transients that closely resembled action-potential–evoked calcium transients observed in previous in vivo studies (Waters and Helmchen 2004; Waters et al. 2003). Interestingly, when we analyzed the spatial profile of calcium transient amplitudes (normalized to the most proximal recording site), we found a variable degree of attenuation, even for events in the same recordings (Fig. 6*C*). Although some calcium transients were almost completely attenuated in the most distal part of the dendrite, others obviously spread much farther distally (Fig. 6, *D* and *E*). This variability was not due to movement artifacts. Rather, this finding is consistent with the idea that action-potential–evoked calcium transients are small in the distal dendrite unless they are boosted by coincident distal synaptic input or during ongoing spontaneous activity (Waters and Helmchen 2004; Waters et al. 2003).

3D ribbon scanning from multiple pyramidal cell dendrites

Finally, we aimed at simultaneous imaging of spatiotemporal activity in multiple apical dendrites of neocortical neurons. To this end we devised a ribbon-like, user-defined scan pattern that creates a fluorescence image of a convoluted plane in 3D space. The principal idea is to define two horizontal free linescans at two different focal depths and to interpolate linearly between these two lines assuming a sawtooth-like z-scan signal (Fig. 7, *A* and *B*; see METHODS). By appropriately selecting dendritic cross sections the 3D ribbon could be adjusted to include several (typically 5–10) dendrites with variable orientations. Figure 7*B* shows an example of a 3D ribbon scan through 10 apical dendrites of neocortical pyramidal neurons, filled with OGB-1 by local electroporation. In the unfolded ribbon, individual dendrites appeared as bright, vertical lines (Fig. 7*B*). Spontaneous cal-

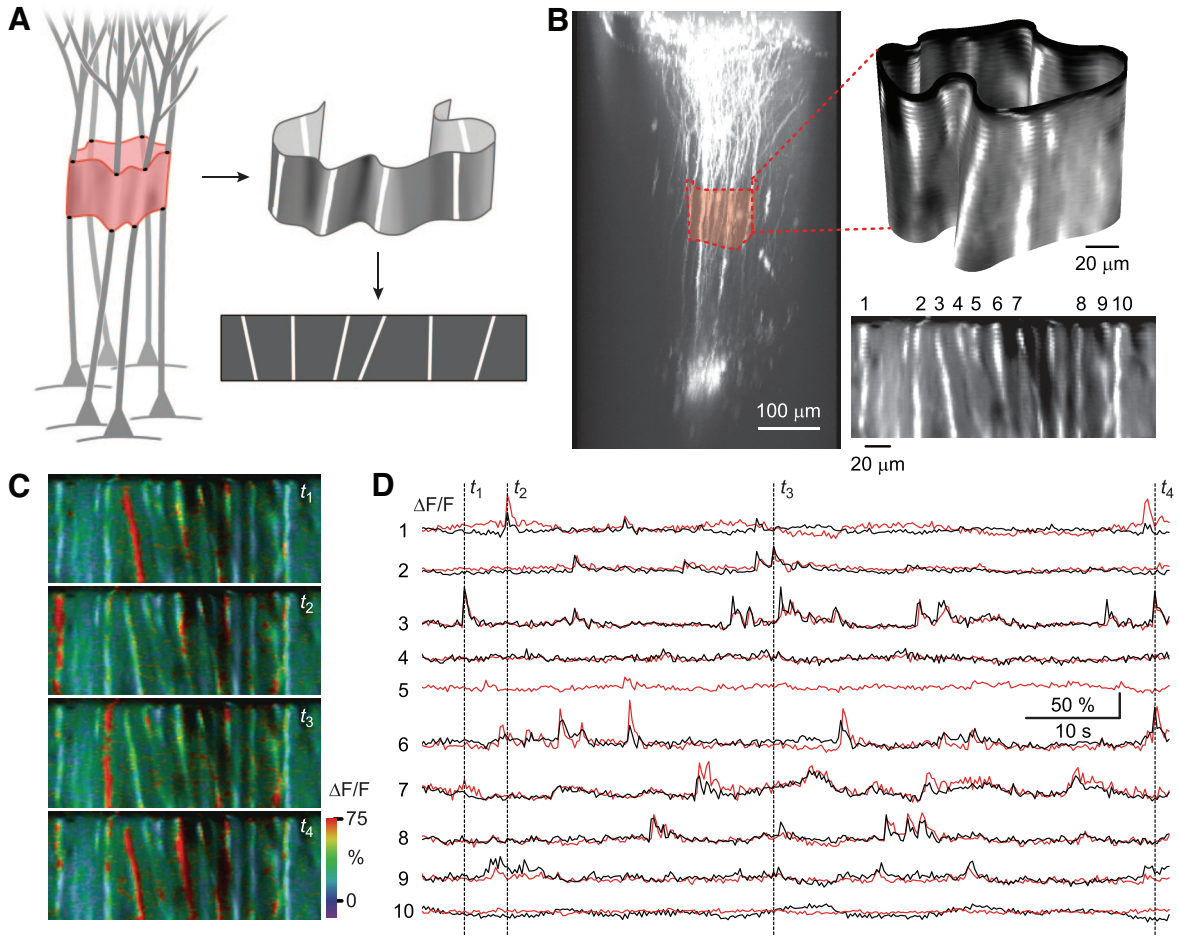

FIG. 7. 3D ribbon scanning of neocortical dendrites. *A*: scheme of scan ribbon pattern enclosing the apical trunks of several dendrites (*left*). Partially unfolded (*top right*) and completely unfolded (*bottom right*) scan ribbon. Dendrites appear as bright, slightly tilted vertical lines. *B*: sideways reconstruction of labeled layer 2/3 neurons stained with the calcium indicator OGB-1 by local electroporation in about 450-μm depth (*left*). Location of a ribbon scan is indicated in red. Actual ribbon-type scan pattern (*top*) and its unfolded version (*bottom*) are both shown on the *right*. Individual dendrites are clearly discernible. *C*: 4 example ΔF/F images showing activity in different dendrites. *D*: time course of spontaneous calcium signals from identified dendrites (ordering indicated in *B*). Signals from proximal (black) and distal (red) regions are shown separately.

cium transients measured simultaneously in the various dendrites were directly visualized (Fig. 7*C*; supplemental movie 5) and analyzed separately for the more proximal and distal segments, respectively (Fig. 7*D*). Similar results were obtained with 3D ribbon scanning in three animals with frame rates $\leq$8 Hz and axial ranges $\leq$100 μm.

DISCUSSION

We have presented novel laser-scanning modes for two-photon microscopy that provide new viewing angles on neural dynamics in vivo. The new scanning modes are especially well suited for imaging dendritic signaling because they enable spatially resolved functional measurements from vertically oriented dendrites. Specifically, we have demonstrated sideways imaging of dendritic calcium signals in cerebellar Purkinje cells, vertical scanning along neocortical pyramidal cell dendrites, and simultaneous calcium imaging along multiple apical dendrites of neocortical pyramidal cells using 3D ribbon scanning. The ability to optically record spatiotemporal patterns of dendritic excitation in vivo will facilitate further studies of dendritic integration in the intact brain.

Arbitrary modes of laser scanning

Our study demonstrates how beneficial novel nonraster-like imaging schemes can prove for experimental studies of neural dynamics. Traditionally, laser-scanning microscopes mostly use raster-like scanning in the *x*–*y* plane—normal to the optical axis—combined with stepwise focal changes for the acquisition of image stacks. Typically, a compromise has to be made between scanning of a single or few structures of interest at high speed (e.g., using linescans) and a more extensive sampling of many structures albeit at reduced speed. For fast imaging reseachers still adhere to 2D imaging, which provides only a limited view on the 3D organized cellular circuits.

Recently, we have introduced a simple 3D laser-scanning approach that collects fluorescence signals along a predefined 3D scan trajectory and thereby enables 10-Hz measurements from populations of several hundred cells in volumes of $\leq$250-μm side length (Göbel et al. 2007). The key element of our two-photon microscope setup is the piezoelectric focusing element, which is used equivalently to the two galvanometric scan mirrors. Axial scanning of a piezoelectrically driven objective has been described previously for *x*–*z*-scanning in confocal and two-photon microscopy (Callamaras and Parker

1999a; Nguyen et al. 2001). However, only one study reported elementary calcium release events in oocytes using this method (Callamaras and Parker 1999b). Here we extended this approach to arbitrary plane imaging in 3D space, which permits optimal adjustment of the viewing angle for imaging particular structures of interest. We exemplified the advantage of this method by performing in vivo calcium imaging in the cerebellar cortex. The same approach should be useful for functional imaging in many other areas of the brain as well as in other research fields such as immunology, dermatology, or cancer research (Helmchen and Denk 2005; Zipfel et al. 2003). Here we applied rather slow frame rates of 2–10 Hz in *x–z*-imaging mode. In principle frame rates of 20 Hz or even video rate should be possible (Göbel et al. 2007; Nguyen et al. 2001).

In our further approach we departed from straight linescans or planar imaging by employing user-defined curved linescans or convoluted image planes. Horizontal free linescans permitted rapid measurements from multiple apical dendrites. Such measurements are flexible and fast, with line durations of only a few milliseconds. They promise to enable detailed investigation of the variability and the synchrony of dendritic excitation in neighboring neurons, particularly in response to sensory input. As a complementary technique we demonstrated user-defined vertical linescans along individual pyramidal cell dendrites. We could achieve acquisition rates of 20 Hz, which should be sufficient to study spatiotemporal profiles of dendritic calcium signaling. Finally, we combined these two approaches and devised the 3D ribbon scan technique, which can spatially resolve calcium signals in multiple, arbitrarily oriented dendrites. In summary, these "free" modes of laser scanning, although generally applicable, are especially suited for in vivo studies of dendritic signaling.

Although alternative laser-scanning technologies are currently being explored for fast and comprehensive 3D imaging, such as axial scanning using acousto-optical deflectors (AODs) (Reddy and Saggau 2005) or fast addressing of optical fibers (Rozsa et al. 2007), these methods have not yet been applied to the study of neural dynamics. The main advantages of our approach are that it is simple and that it lacks any additional optical aberrations.

Functional imaging of dendrites in vivo

Fluorescence imaging of ion concentrations or biochemical activity has been extremely useful for characterizing intrinsic excitability and synaptic integration in dendrites of various cell types. Following the first demonstration of functional dendritic imaging in the mammalian brain in vivo (Svoboda et al. 1997), several obstacles prevented widespread use of this technique. Besides the high cost of a two-photon microscope, calcium indicator labeling in vivo 10 years ago relied on intracellular filling of individual neurons by an electrode, which still is a demanding task. Consequently, only few studies succeeded in characterizing action-potential–evoked calcium transients in dendrites of neocortical pyramidal neurons (Helmchen et al. 1999; Svoboda et al. 1997, 1999; Waters and Helmchen 2004; Waters et al. 2003) and of mitral cells in the olfactory bulb (Charpak et al. 2001; Debarbieux et al. 2003). Meanwhile, several new in vivo labeling methods have become available, including bulk loading of membrane-permeable calcium dyes (Kerr et al. 2005; Stosiek et al. 2003; Sullivan et al. 2005), electroporation (Nagayama et al. 2007; Nevian and Helmchen 2007), and the expression of genetically encoded calcium indicators (Diez-Garcia et al. 2007; Hasan et al. 2004; Heim et al. 2007; Miyawaki 2005). These advances, together with the flexible 3D scanning modes presented here, should enable far more detailed studies of dendritic activation patterns in the intact brain.

So far most in vivo studies have focused on dendritic calcium signals evoked by action potentials. Far less is known about calcium signaling in the subthreshold regime. Axial scanning modes may facilitate the search for localized dendritic calcium signals because they might be induced by specific synaptic activation patterns. In the neocortex, individual dendritic branches might generate local dendritic spikes under certain conditions acting as isolated functional units (Gulledge et al. 2005; Holthoff et al. 2006; Polsky et al. 2004). Moreover, it is unclear when dendritic calcium waves induced by release of calcium from intracellular stores (Ross et al. 2005) might occur in the intact brain. In the cerebellar cortex, it might be possible to resolve natural activation patterns in both parallel fibers and Purkinje cell dendrites, e.g., on sensory stimulation. Local dendritic calcium signals in Purkinje cells have been implicated in various forms of synaptic integration and plasticity (Hartmann and Konnerth 2005) but so far have resisted investigations in vivo. Moreover, Purkinje cells display complex dynamics comprising bistability (Loewenstein et al. 2005) that could be further analyzed using the imaging techniques presented here. Similar questions could also be addressed in mitral cells in the olfactory bulb (Charpak et al. 2001; Nagayama et al. 2007).

Finally, novel laser-scanning technologies may not only provide means to read out neuronal signals. Patterned photostimulation could in addition be used to purposely impose activation patterns on single cells (Shoham et al. 2005) or cellular circuits (Arenkiel et al. 2007), in particular using genetically encoded optical switches (Zhang et al. 2007). We therefore expect that the presented 3D scanning approaches will be powerful tools to dissect fundamental mechanisms of neural circuit function.

ACKNOWLEDGMENTS

We thank U. Gerber, M. E. Larkum, W. N. Ross, and S. S.-H. Wang for discussions and comments on the manuscript. We are grateful to S. Giger, E. Hochreutener, and H. Kasper for expert technical assistance.

GRANTS

This work was supported by grants from the Human Frontier Science Program and the Swiss National Science Foundation to F. Helmchen and by a doctoral fellowship from the Center for Neuroscience Zurich to W. Göbel.

REFERENCES

Arenkiel BR, Peca J, Davison IG, Feliciano C, Deisseroth K, Augustine GJ, Ehlers MD, Feng G. In vivo light-induced activation of neural circuitry in transgenic mice expressing channelrhodopsin-2. *Neuron* 54: 205–218, 2007.

Callamaras N, Parker I. Construction of a confocal microscope for real-time *x-y* and *x-z* imaging. *Cell Calcium* 26: 271–279, 1999a.

Callamaras N, Parker I. Radial localization of inositol 1,4,5-trisphosphate-sensitive Ca^{2+} release sites in Xenopus oocytes resolved by axial confocal linescan imaging. *J Gen Physiol* 113: 199–213, 1999b.

Charpak S, Mertz J, Beaurepaire E, Moreaux L, Delaney K. Odor-evoked calcium signals in dendrites of rat mitral cells. *Proc Natl Acad Sci USA* 98: 1230–1234, 2001.

Debarbieux F, Audinat E, Charpak S. Action potential propagation in dendrites of rat mitral cells in vivo. *J Neurosci* 23: 5553–5560, 2003.

Denk W, Strickler JH, Webb WW. Two-photon laser scanning fluorescence microscopy. *Science* 248: 73–76, 1990.

Diez-Garcia J, Akemann W, Knöpfel T. In vivo calcium imaging from genetically specified target cells in mouse cerebellum. *Neuroimage* 34: 859–869, 2007.

Göbel W, Kampa BM, Helmchen F. Imaging cellular network dynamics in three dimensions using fast 3D laser scanning. *Nat Methods* 4: 73–79, 2007.

Gulledge AT, Kampa BM, Stuart GJ. Synaptic integration in dendritic trees. *J Neurobiol* 64: 75–90, 2005.

Hartmann J, Konnerth A. Determinants of postsynaptic Ca^{2+} signaling in Purkinje neurons. *Cell Calcium* 37: 459–466, 2005.

Hasan MT, Friedrich RW, Euler T, Larkum ME, Giese G, Both M, Duebel J, Waters J, Bujard H, Griesbeck O, Tsien RY, Nagai T, Miyawaki A, Denk W. Functional fluorescent Ca^{2+} indicator proteins in transgenic mice under TET control. *PLoS Biol* 2: e163, 2004.

Häusser M, Spruston N, Stuart GJ. Diversity and dynamics of dendritic signaling. *Science* 290: 739–744, 2000.

Heim N, Garaschuk O, Friedrich MW, Mank M, Milos RI, Kovalchuk Y, Konnerth A, Griesbeck O. Improved calcium imaging in transgenic mice expressing a troponin C-based biosensor. *Nat Methods* 4: 127–129, 2007.

Helmchen F, Denk W. Deep tissue two-photon microscopy. *Nat Methods* 2: 932–940, 2005.

Helmchen F, Svoboda K, Denk W, Tank DW. In vivo dendritic calcium dynamics in deep-layer cortical pyramidal neurons. *Nat Neurosci* 2: 989–996, 1999.

Helmchen F, Waters J. Ca^{2+} imaging in the mammalian brain in vivo. *Eur J Pharm* 447: 119–129, 2002.

Holthoff K, Kovalchuk Y, Konnerth A. Dendritic spikes and activity-dependent synaptic plasticity. *Cell Tissue Res* 326: 369–377, 2006.

Iyer V, Hoogland TM, Saggau P. Fast functional imaging of single neurons using random-access multiphoton (RAMP) microscopy. *J Neurophysiol* 95: 535–545, 2006.

Keating JG, Thach WT. No clock signal in the discharge of neurons in the deep cerebellar nuclei. *J Neurophysiol* 77: 2232–2234, 1997.

Kerr JN, Greenberg D, Helmchen F. Imaging input and output of neocortical networks in vivo. *Proc Natl Acad Sci USA* 102: 14063–14068, 2005.

Kleinfeld D, Mitra PP, Helmchen F, Denk W. Fluctuations and stimulus-induced changes in blood flow observed in individual capillaries in layers 2 through 4 of rat neocortex. *Proc Natl Acad Sci USA* 95: 15741–15746, 1998.

Kurtz R, Fricke M, Kalb J, Tinnefeld P, Sauer M. Application of multiline two-photon microscopy to functional in vivo imaging. *J Neurosci Methods* 151: 276–286, 2006.

Loewenstein Y, Mahon S, Chadderton P, Kitamura K, Sompolinsky H, Yarom Y, Häusser M. Bistability of cerebellar Purkinje cells modulated by sensory stimulation. *Nat Neurosci* 8: 202–211, 2005.

Miyakawa H, Lev-Ram V, Lasser-Ross N, Ross WN. Calcium transients evoked by climbing fiber and parallel fiber synaptic inputs in guinea pig cerebellar Purkinje neurons. *J Neurophysiol* 68: 1178–1189, 1992.

Miyawaki A. Innovations in the imaging of brain functions using fluorescent proteins. *Neuron* 48: 189–199, 2005.

Nagayama S, Zeng S, Xiong W, Fletcher ML, Masurkar AV, Davis DJ, Pieribone VA, Chen WR. In vivo simultaneous tracing and Ca^{2+} imaging of local neuronal circuits. *Neuron* 53: 789–803, 2007.

Nevian T, Helmchen F. Calcium indicator loading of neurons using single-cell electroporation. *Pfluegers Arch* 454: 675–688, 2007.

Nguyen QT, Callamaras N, Hsieh C, Parker I. Construction of a two-photon microscope for video-rate Ca^{2+} imaging. *Cell Calcium* 30: 383–393, 2001.

Pichitpornchai C, Rawson JA, Rees S. Morphology of parallel fibres in the cerebellar cortex of the rat: an experimental light and electron microscopic study with biocytin. *J Comp Neurol* 342: 206–220, 1994.

Polsky A, Mel BW, Schiller J. Computational subunits in thin dendrites of pyramidal cells. *Nat Neurosci* 7: 621–627, 2004.

Reddy GD, Saggau P. Fast three-dimensional laser scanning scheme using acousto-optic deflectors. *J Biomed Opt* 10: 64038, 2005.

Ross WN, Nakamura T, Watanabe S, Larkum M, Lasser-Ross N. Synaptically activated Ca^{2+} release from internal stores in CNS neurons. *Cell Mol Neurobiol* 25: 283–295, 2005.

Rozsa B, Katona G, Vizi ES, Varallyay Z, Saghy A, Valenta L, Maak P, Fekete J, Banyasz A, Szipocs R. Random access three-dimensional two-photon microscopy. *Appl Opt* 46: 1860–1865, 2007.

Salome R, Kremer Y, Dieudonne S, Leger JF, Krichevsky O, Wyart C, Chatenay D, Bourdieu L. Ultrafast random-access scanning in two-photon microscopy using acousto-optic deflectors. *J Neurosci Methods* 154: 161–174, 2006.

Shoham S, O'Connor DH, Sarkisov DV, Wang SS. Rapid neurotransmitter uncaging in spatially defined patterns. *Nat Methods* 2: 837–843, 2005.

Stosiek C, Garaschuk O, Holthoff K, Konnerth A. In vivo two-photon calcium imaging of neuronal networks. *Proc Natl Acad Sci USA* 100: 7319–7324, 2003.

Sullivan MR, Nimmerjahn A, Sarkisov DV, Helmchen F, Wang SS-H. In vivo calcium imaging of circuit activity in cerebellar cortex. *J Neurophysiol* 94: 1636–1644, 2005.

Svoboda K, Denk W, Kleinfeld D, Tank DW. In vivo dendritic calcium dynamics in neocortical pyramidal neurons. *Nature* 385: 161–165, 1997.

Svoboda K, Helmchen F, Denk W, Tank DW. Spread of dendritic excitation in layer 2/3 pyramidal neurons in rat barrel cortex in vivo. *Nat Neurosci* 2: 65–73, 1999.

Waters J, Helmchen F. Boosting of action potential backpropagation by neocortical network activity in vivo. *J Neurosci* 24: 11127–11136, 2004.

Waters J, Larkum M, Sakmann B, Helmchen F. Supralinear Ca^{2+} influx into dendritic tufts of layer 2/3 neocortical pyramidal neurons in vitro and in vivo. *J Neurosci* 23: 8558–8567, 2003.

Yuste R, Majewska A, Holthoff K. From form to function: calcium compartmentalization in dendritic spines. *Nat Neurosci* 3: 653–659, 2000.

Yuste R, Tank DW. Dendritic integration in mammalian neurons, a century after Cajal. *Neuron* 16: 701–716, 1996.

Zhang F, Wang LP, Brauner M, Liewald JF, Kay K, Watzke N, Wood PG, Bamberg E, Nagel G, Gottschalk A, Deisseroth K. Multimodal fast optical interrogation of neural circuitry. *Nature* 446: 633–634, 2007.

Zipfel WR, Williams RM, Webb WW. Nonlinear magic: multiphoton microscopy in the biosciences. *Nat Biotechnol* 21: 1369–1377, 2003.